The Kondo effect in amorphous $Si_{1-c}Mn_c$

1997 J. Phys.: Condens. Matter 9 499

(http://iopscience.iop.org/0953-8984/9/2/017)

J. Phys.: Condens. Matter **9** (1997) 499–506. Printed in the UK PII: S0953-8984(97)75002-1

The Kondo effect in amorphous $Si_{1-c}Mn_c$

A I Yakimov†‖, A V Dvurechenskii‡, C J Adkins† and V A Dravin§

† Cavendish Laboratory, University of Cambridge, Madingley Road, Cambridge CB3 0HE, UK
‡ Institute of Semiconductor Physics, 630090 Novosibirsk, Russia
§ P N Lebedev Physical Institute, 117924 Moscow, Russia

Received 31 May 1996, in final form 17 October 1996

Abstract. We present conductivity data for a range of a-$Si_{1-c}Mn_c$ films on the metallic side of the metal–insulator transition. In the temperature range $T = 20$–200 K, electron–electron interaction and weak-localization effects are identified, with the temperature dependence of the latter resulting from inelastic electron–electron scattering. At lower temperatures, we have observed a deviation from the high-T behaviour towards higher resistance. This effect is attributed to Kondo-type s–d exchange scattering of conduction electrons by Mn spins.

1. Introduction

It is well known for metals that the presence of magnetic moments significantly affects the electrical resistivity. Magnetic properties of semiconductors are less studied and not nearly as well understood as those of metals. Investigations of hopping conductivity on the insulating side of the metal–insulator transition (MIT) in amorphous a-$Si_{1-c}Mn_c$ alloys ($c < 0.13$) obtained by ion implantation of Mn have revealed a 'hard' magnetic gap in the density of localized states at low temperatures (Yakimov *et al* 1995). This modification of the electron spectrum is caused by the s–d exchange interaction between the hopping electrons and localized spins on the Mn atoms with the formation of magnetic polarons. The aim of the present work is to establish the role of magnetic effects on the opposite side of the MIT where the conduction is metallic.

2. Experimental details

Five a-$Si_{1-c}Mn_c$ samples ($c = 0.14$–0.22) were produced by room temperature implantation of Mn ion doses of the order of 10^{17} cm^{-2} into crystalline Si films (0.4 μm thick) on sapphire. Because of its large thermal conductivity, this substrate prevents overheating of the silicon layer during irradiation. The density of the ion current was about 7 mA cm^{-2}. A homogeneous distribution of the impurity across the film thickness was ensured by varying the ion energy in the range 20–300 keV. Figure 1 shows a Monte Carlo computation of the Mn distribution for the sample with $c = 0.18$. The Mn implantation results both in amorphization and doping of the Si film. The details of sample preparation can be found in the work of Dvurechenskii and Yakimov (1989). For electrical measurements, the thin-film samples were scribed to define a conductive channel with resistance sidebars. The resistivity was measured as a function of temperature between 4 K and 200 K by four-terminal ac techniques using a lock-in amplifier at a frequency of 111 Hz.

‖ Present address: Institute of Semiconductor Physics, 630090 Novosibirsk, Russia.

0953-8984/97/020499+08$19.50

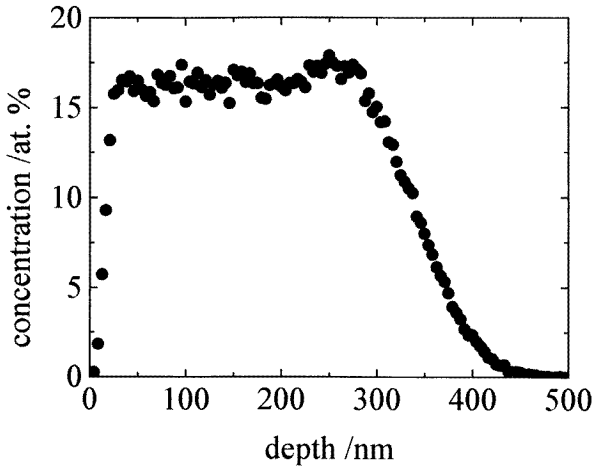

Figure 1. A Monte Carlo computation of the Mn distribution in the $c = 0.18$ silicon film after implantation.

3. Experimental results

For disordered solids, the temperature dependence of the conductivity in the metallic regime is determined by quantum corrections to the Boltzmann conductivity σ_B and has the following form for a three-dimensional conductor:

$$\sigma(T) = \sigma_B + aT^{1/2} + bT^p$$

where the second term is due to long-range electron–electron interactions (Altshuler and Aronov 1979) and the final term (the so-called 'weak-localization' correction) is due to quantum interference of electrons (Bergmann 1983, 1984), with $b > 0$ and p having a value determined by the type of scattering: $p = 2$ for phonon scattering below the Debye temperature and $p = 1$ for electron–electron scattering (Mott 1990).

The conductivity data are shown in figure 2(a). The procedure that we have generally used, in exploring for the best functional representation of our data, is to fit data to the form

$$\sigma = \sigma(0) + aT^q + bT^p \tag{1}$$

where the first of the temperature-dependent terms is allocated to interaction effects and the second to weak localization. Either index can be set before fitting and some fits were also made with only one temperature-dependent term. Details of fitting for $T > 20$ K are summarized in table 1. Parameters set before fitting are printed in bold type. χ provides a measure of the accuracy with which the fitted equation describes the data. It is defined by

$$\chi = \left\{ \frac{1}{N} \sum_{i=1}^{N} [\sigma_i - \sigma(T_i)]^2 \right\}^{1/2}$$

where N is the number of data points, σ_i are the measured values and $\sigma(T_i)$ the values calculated from the fitted equation. Clearly, minimum values of χ correspond to the best fits. It is evident from table 1 that all attempts at fitting produce a positive $\sigma(0)$, and hence these samples do lie on the metal side of the MIT. Extrapolation of the conductivity data to zero temperature suggests that the transition occurs at $c \approx 0.13$. This is in agreement with the result obtained from the insulator side of the transition (Dvurechenskii and Yakimov

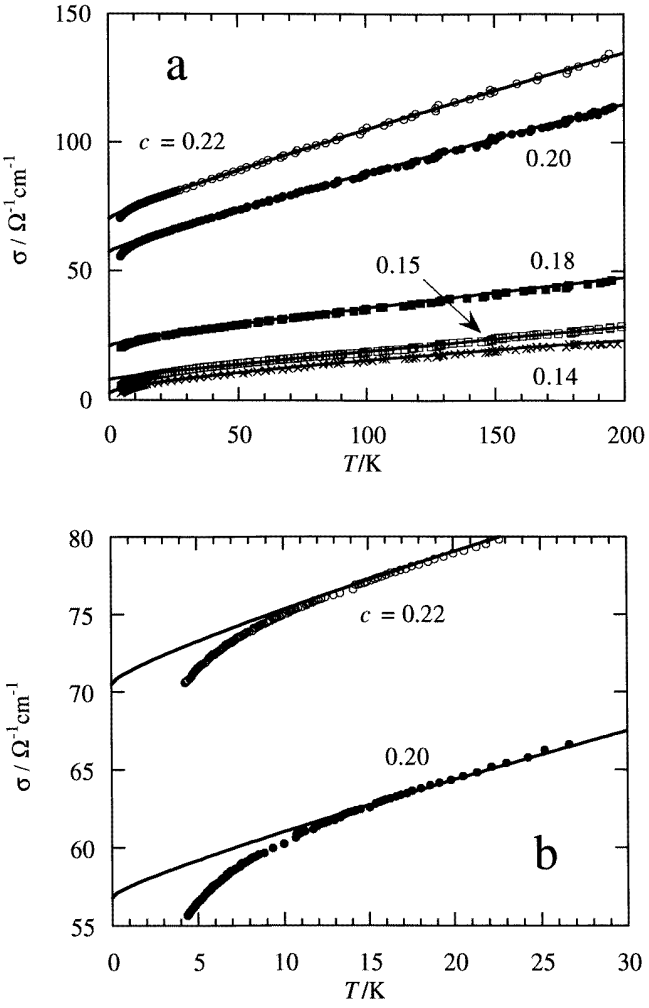

Figure 2. (a) Conductivity as a function of temperature for all samples. (b) An expanded view of the low-temperature conductivity for samples with $c = 0.22$ and 0.20. The solid lines in both figures ((a) and (b)) are the best fits to equation (1) in the temperature range 20–200 K.

1989). Solid lines in figure 2(a) represent the best fits which correspond to the minimum of χ in table 1.

We can check the validity of the weak-localization model applied here by extracting the value of inelastic diffusion length L_i. We do this for the sample with the highest Mn concentration for which this model should produce the most reasonable results. Inelastic scattering introduces random fluctuations in the time evolution of an electronic state. Such fluctuations limit the quantum interference necessary for localization and hence enhance the system conductivity by a value of $\delta\sigma(T) = e^2/(2\pi^2\hbar L_i)$ (Lee and Ramakrishnan 1985). This term corresponds to $\delta\sigma(T) = bT^p$ in equation (1). So, we have $L_i = e^2/(2\pi^2\hbar bT^p)$ which gives a quite acceptable result: $L_i = 36$ nm at $T = 10$ K.

We conclude that the results (>20 K) for our most metallic samples ($c \geqslant 0.15$) are satisfactorily explained by a positive electron–electron interaction term with a weak-

Table 1. The algebraic fitting of the conductivity in the temperature range 20–200 K. The table shows the parameters obtained by least-squares fitting to the form $\sigma = \sigma(0) + at^q + bT^p$. Parameters in bold type were fixed prior to fitting. c is the Mn concentration.

c	$\sigma(0)/\Omega^{-1}$ cm^{-1}	a/Ω^{-1} cm^{-1} K^{-q}	q	b/Ω^{-1} cm^{-1} K^{-p}	p	χ/Ω^{-1} cm^{-1}
0.22	71.6	0.26	0.75	0.26	**1**	1.47
	70.9	0.52	0.91	**0**	—	0.47
	70.2	0.41	**0.50**	0.41	0.95	0.44
	70.2	0.43	0.52	0.39	0.94	0.44
0.20	58.3	0.26	0.64	0.26	**1**	1.96
	57.03	0.51	0.89	**0**	—	0.67
	57.3	0.38	**0.5**	0.33	0.96	0.56
	56.9	0.42	0.49	0.39	0.93	0.56
0.18	22.4	0.1	0.75	0.1	**1**	0.8
	19.8	0.52	0.73	**0**	—	0.61
	21.0	0.35	0.23	0.26	0.87	0.57
	21.1	0.30	**0.50**	0.17	0.93	0.55
0.15	5.2	0.66	0.66	**0**	—	0.48
	8.3	0.35	−1.35	0.17	0.90	0.36
	8.6	0.08	0.75	0.08	**1**	0.27
	8.0	0.25	**0.50**	0.09	1.0	0.25
0.14	9.7	0.12	−0.85	0.12	**1**	8.29
	2.9	0.003	**0.50**	0.53	0.69	0.51
	2.9	−0.05	0.72	0.59	0.69	0.48
	3.5	0.44	0.71	**0**	—	0.36

localization term mediated by inelastic electron–electron scattering (corresponding to $p \approx 1$).

The 14% sample behaves differently. Putting $q = 0.5$ gives a poor fit with a large value of χ. The best fit is obtained with $q = 0.71$ putting $b = 0$. We suppose that this sample lies in the critical region of MIT. Kaveh *et al* (1987) have shown that very near the MIT in a three-dimensional system, the inelastic diffusion length is reduced and may become the smallest length scale (even smaller than the interaction length). In this case, the term due to quantum interference tends to $T^{3/4}$ (Kaveh and Wiser (1984), p 273).

One can see in figure 2(a) that at low temperatures ($T < 10$–20 K) the conductivity deviates from (1) and starts to decrease more rapidly as temperature is reduced. Figure 2(b) shows an expanded view for the $c = 0.22$ and 0.20 samples at $T < 30$ K. Note that experimental values of $\sigma(T = 4.2\ \text{K})$ are less than $\sigma(0)$ extracted from the fitting procedure. Figure 3(a) demonstrates the best fit of the low-temperature data for $c = 0.22$ to equation (1) (broken line). Clearly, the agreement is very poor. Systematic deviations from (1) indicate that a new conduction mechanism, not taken into consideration in (1) and reducing σ towards lower temperature, needs to be considered.

Analysis shows that the low-temperature conductivity can be better described by a logarithmic dependence. The solid line in figure 3(a) is a least-squares fit to the $\sigma = \sigma_0 + A \ln T$ form. The dependences $\sigma(\ln T)$ at $T < 20$ K are plotted for all samples in figure 3(b). Data for $c = 0.14$–0.20 are displaced vertically for clarity. The validity of the $\ln T$ law is apparent. One possible explanation for logarithmic behaviour could be a decrease of the system dimensionality from 3 to 2. The effective dimensionality of the system is the number of dimensions for which the system size is larger than the inelastic and/or interaction lengths. Since both of them are functions of temperature, one can cross over from three- (3D) to two-dimensional (2D) behaviour for a given film on cooling. In

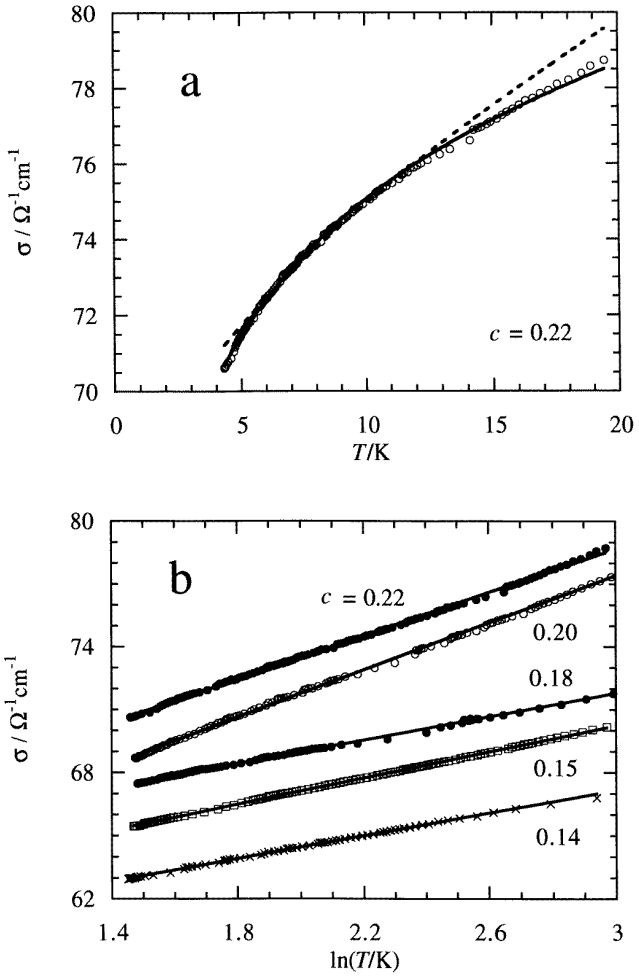

Figure 3. (a) The conductivity as a function of temperature at $T < 20$ K for the $c = 0.22$ sample. The broken line is the best fit to equation (1) in the temperature range 4–20 K. The solid line represents the best fit to the logarithmic form. (b) The conductivity as a function of $\ln T$.

2D conductors, both interaction and weak-localization terms have a logarithmic dependence on temperature (see Lee and Ramakrishnan (1985) and references therein); but in contrast with the 3D case, in 2D systems the magnitude of the quantum corrections is universal and has a value of about $G_0 = e^2/2\pi^2\overline{h} \approx 10^{-5}\ \Omega^{-1}$. We have re-calculated the conductivity data to obtain two-dimensional conductance and found that in our samples the value of the pre-logarithmic factor is one order of magnitude larger than G_0. Another discrepancy with the 2D model arises from the fact that the inelastic diffusion length L_i of 36 nm at 10 K estimated from the high-temperature 3D behaviour seems to be small compared with the film thickness, 300 nm.

The low-temperature anomaly leads to a decrease of conductivity in relation to the high-T behaviour. This means that an additional resistivity mechanism becomes important. We attribute this channel to s–d scattering of conduction electrons from localized magnetic

Table 2. Fitting of the resistivity deviation data in the temperature range 4–20 K: the table shows the parameters obtained by least-squares fitting to the form $\rho = \rho_0 + \rho_1[1 + (J/n)g(\epsilon_F)\ln(\epsilon_F/kT)]^{-2}$. The parameters n, $g(\epsilon_F)$ and ϵ_F were calculated independently and fixed before fitting.

c	$n/10^{22}$ cm^{-3}	ϵ_F/eV	$g(\epsilon_F)/10^{21}$ eV^{-1} cm^{-3}	ρ_0/mΩ cm	ρ_1/mΩ cm	J/eV
0.14	1.4	3.46	3.0	−31.7	1.64	−0.45
0.15	1.5	3.6	3.15	−16.4	1.35	−0.45
0.18	1.8	4.08	3.4	−1.43	0.13	−0.47
0.20	2.0	4.37	3.53	−0.53	0.04	−0.46
0.22	2.2	4.66	3.64	−0.3	0.02	−0.49

moments of the impurity Mn atoms associated with the half-filled 3d shell. The behaviour of an electron gas exchange coupled to the spin of the paramagnetic impurities in metals was originally considered by Kondo (1964). In the first Born approximation, an allowance for the scattering gives rise to a constant correction to the total resistivity. However, in the next approximation, the exchange scattering is found to depend on the electron energy and, therefore, on kT. Energetic considerations suggest that the carrier electron spin should be antiparallel to the magnetic moment of the impurity and that scattering has to be accompanied by two spin flips. An elegant explanation of this process for a singlet state was given by Mott (Mott (1990), p 104). A conduction electron from near the Fermi energy ϵ_F jumps onto the impurity with spin antiparallel to that of the electron already there. The level becomes doubly occupied. Then the other electron from the impurity jumps rapidly back to a state at the Fermi energy of the metal. The Kondo effect results in the following correction to the resistivity of a metal:

$$\rho_{spin} = c\rho_1[1 - 2(J/n)g(\epsilon_F)\ln(\epsilon_F/kT)] \tag{2}$$

where J is the exchange integral, n is the electron density and $g(\epsilon_F)$ is the density of states near the Fermi level. Equation (2) contains a singular term involving $\ln T$ which increases towards low temperature provided that the s–d exchange integral is negative (antiferromagnetic coupling). This term arises from the second Born approximation as a result of the dynamical nature of the spin system. Its singularity is associated with the sharpness of the Fermi surface.

Since the Kondo scattering term adds to other scattering mechanisms, we must analyse the deviation from the high-temperature *resistivity* (not conductivity): $\rho_K(T) = \rho_{ex} - 1/[\sigma(0) + aT^q + bT^p]$, where ρ_{ex} is the total low-temperature resistivity measured in the experiment. The value of ρ_K is plotted as a function of $\ln T$ in figure 4. Although the agreement at higher temperatures is good, one can see that there is a strong deviation from simple $\ln T$ dependence towards lower temperatures. This is more evident for samples with lower Mn concentration. At high temperatures the impurities behave like free (paramagnetic) moments. However, below a characteristic temperature, specific for each alloy system, the impurity becomes non-magnetic due to its interaction with the conduction electrons. This signifies the breakdown of higher-order perturbation theory which is used to calculate the physical properties from the s–d Hamiltonian. At low T, the appearance of logarithmic divergences denotes a broad temperature transition to a quasi-bound state (Mydosh and Nieuwenhuys 1980) which possesses an enhanced electron scattering cross-section. Abrikosov (1965) and Suhl (1965) summed the most divergent terms in perturbation theory expansions and showed that at low temperatures

$$\rho = \rho_0 + c\rho_1[1 + (J/n)g(\epsilon_F)\ln(\epsilon_F/kT)]^{-2}. \tag{3}$$

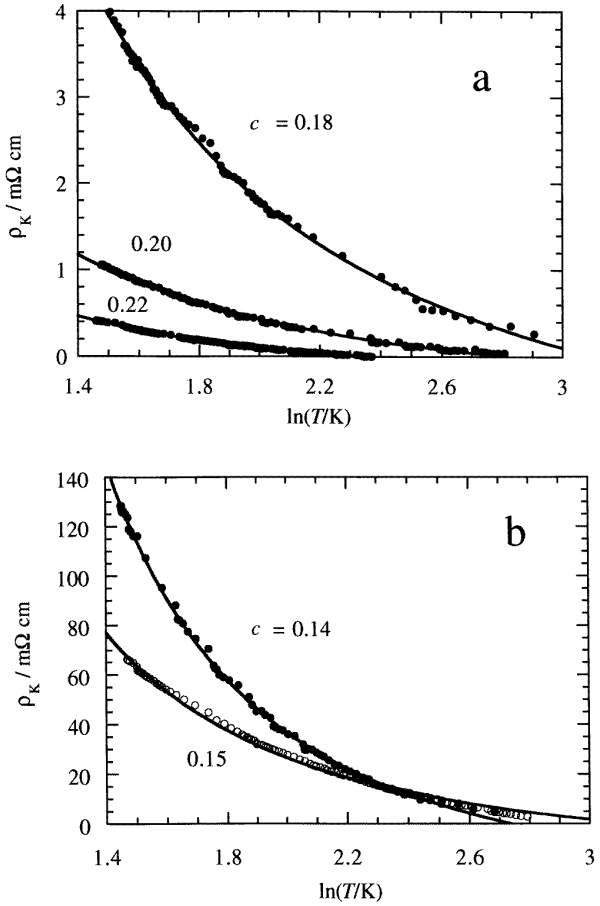

Figure 4. The low-temperature excess resistivity as a function of $\ln T$ for different samples. The solid lines are the best fits to equation (3).

To make fitting calculations using form (3) we reduced the number of free parameters by choosing the appropriate values of ϵ_F and $g(\epsilon_F)$. The value of the Fermi energy is given by

$$\epsilon_F = \hbar^2(3\pi^2 n)^{2/3}/(2m^*) \tag{4}$$

where m^* is the electron effective mass. The density of states can be calculated from

$$g(\epsilon_F) = \frac{m^*}{\hbar^2}\left(\frac{3n}{8\pi^4}\right)^{1/3}. \tag{5}$$

Values of ϵ_F and $g(\epsilon_F)$ were set before fitting and the best fits then yielded values for ρ_0, ρ_1 and J which are summarized in table 2. Here we used $m^* = 0.4m_0$ (Yakimov *et al* 1996) and n is twice the Mn concentration (corresponding to a valence of 2). Clearly, the magnitude obtained for the exchange integral, $J \approx -0.45$ eV, is quite reasonable and supports our interpretation. The negative value of ρ_0 can be easily understood as follows. Equation (3) contains contributions from the potential scattering from the magnetic impurities and the exchange scattering obtained in the first Born approximation. Since both of them are temperature independent they have been already included in the $\sigma(0)$ term. So, these contributions should be subtracted from (3).

The Kondo effect has been the subject of extensive experimental research in crystalline metals. Intentional doping of semiconductors with magnetic impurities is usually difficult because most magnetic impurities form deep energy levels and thus are not able to produce a metallic state. In amorphous semiconductors, such as silicon, this problem is absent. It is possible to introduce the metallic impurities with concentrations comparable with the concentration of the host atoms. Furthermore, many studies (Hasegawa and Tsuei 1971, Liang and Tsuei 1971, 1973) have shown that a relatively large concentration of a magnetic impurity can be introduced in amorphous alloys without quenching the s–d exchange scattering through d–d spin correlation between magnetic atoms. All of these facts make amorphous semiconductors attractive for investigation of the Kondo effect.

4. Conclusions

We have presented three-dimensional conductivity results for a range of a-$Si_{1-c}Mn_c$ alloys on the metallic side of the metal–insulator transition. In the temperature range 20–200 K, we identify contributions to the conductivity from weak-localization and electron–electron interactions. The temperature dependence of the weak-localization term implies dominance of inelastic electron–electron scattering. At lower temperatures ($<$20 K), we have observed a deviation from the high-T behaviour towards higher resistance. This singularity is attributed to Kondo-type antiferromagnetic interaction of isolated Mn spins with the surrounding conduction electrons. An exchange coupling constant $J \approx -0.45$ eV has been determined from analysis of the experimental data.

Acknowledgments

We thank Jenny Hampton for assistance in the magnetoresistance measurements and Dr E Astrakharchik for very useful discussions of electron transport in the metallic regime. One of the authors (AIY) is grateful to NATO for an Expert Visit Grant (HTECH.EV 951113) that enabled him to carry out the research in Cambridge. The work was supported in part by INTAS (Grant No 94-4435).

References

Abrikosov A A 1965 *Physics* **2** 21
Altshuler B L and Aronov A G 1979 *Solid State Commun.* **30** 115
Bergmann G 1983 *Phys. Rev.* B **28** 2914
——1984 *Phys. Rep.* **107** 1
Dvurechenskii A V and Yakimov A I 1989 *Sov. Phys–JETP* **68** 91
Hasegawa R and Tsuei C C 1971 *Phys. Rev.* B **3** 214
Kaveh M, Newson D J, Ben Zimra D and Pepper M 1987 *J. Phys. C: Solid State Phys.* **20** L19
Kaveh M and Wiser N 1984 *Adv. Phys.* **33** 257
Kondo J 1964 *Prog. Theor. Phys.* **32** 37
Lee P A and Ramakrishnan T V 1985 *Rev. Mod. Phys.* **57** 287
Liang V K C and Tsuei C C 1971 *Solid State Commun.* **9** 579
——1973 *Phys. Rev.* B **7** 3215
Mott N F 1990 *Metal–Insulator Transitions* 2nd edn (London: Taylor and Francis)
Mydosh J A and Nieuwenhuys G J 1980 *Ferromagnetic Materials* ed E P Wohlfarth (Amsterdam: North-Holland)
Suhl H 1965 *Physics* **2** 39
Yakimov A I, Stepina N P, Dvurechenskii A V, Adkins C J and Dravin V A 1996 *Phil. Mag. Lett.* **73** 17
Yakimov A I, Wright T, Adkins C J and Dvurechenskii A V 1995 *Phys. Rev.* B **51** 16 549